Available online at www.sciencedirect.com
SCIENCE DIRECT®
Marine Chemistry 82 (2003) 239–254
MARINE CHEMISTRY
www.elsevier.com/locate/marchem

Tracing dissolved organic matter in aquatic environments using a new approach to fluorescence spectroscopy

Colin A. Stedmon[a,*], Stiig Markager[a], Rasmus Bro[b]

[a] Department of Marine Ecology, National Environmental Research Institute, P.O. Box 358, Frederiksborgvej 399, DK-4000 Roskilde, Denmark
[b] Department of Dairy and Food Science, The Royal Veterinary and Agricultural University, Rolighedsvej 30, DK-1958 Frederiksberg, Denmark

Received 14 August 2002; received in revised form 23 January 2003; accepted 22 April 2003

Abstract

Dissolved organic matter (DOM) is a complex and poorly understood mixture of organic polymers that plays an influential role in aquatic ecosystems. In this study we have successfully characterised the fluorescent fraction of DOM in the catchment of a Danish estuary using fluorescence excitation–emission spectroscopy and parallel factor analysis (PARAFAC). PARAFAC aids the characterisation of fluorescent DOM by decomposing the fluorescence matrices into different independent fluorescent components. The results reveal that at least five different fluorescent DOM fractions present (in significant amounts) in the catchment and that the relative composition is dependent on the source (e.g. agricultural runoff, forest soil, aquatic production). Four different allochthonous fluorescent groups and one autochthonous fluorescent group were identified. The ability to trace the different fractions of the DOM pool using this relatively cheap and fast technique represents a significant advance within the fields of aquatic ecology and chemistry, and will prove to be useful for catchment management.

Keywords: Coloured dissolved organic matter; Fluorescence; Modelling; River; Mixing

1. Introduction

Dissolved organic matter (DOM) plays an integral role in shaping aquatic ecosystems. Its concentration and composition both directly and indirectly influence the biology (microbial and plankton ecology, e.g. Williamson et al., 2001), chemistry (trace metal speciation and transport, e.g. Berault et al., 1996; polycyclic aromatic hydrocarbons (PAHs) toxicity, e.g. Diamond et al., 2000) and physics (optical properties, e.g. Bricaud et al., 1981) of aquatic environments. In many freshwaters and coastal waters, the major source of DOM is the degradation of terrestrial plant matter, which is dissolved and transported through river systems and estuaries to the marine environment. Exudation by aquatic plants and their degradation are also important sources of DOM in natural waters (Nagata, 2002; Carlson, 2002). DOM is a heterogeneous mixture of aliphatic and aromatic polymers and its composition varies in time and space depending on proximity to sources and exposure to degradation processes. To understand the dynamics of DOM in aquatic ecosystems, it is essential to trace the

* Corresponding author. Tel.: +45-4630-1805; fax: +45-4630-1211.
E-mail address: cst@dmu.dk (C.A. Stedmon).

0304-4203/03/$ - see front matter © 2003 Elsevier Science B.V. All rights reserved.
doi:10.1016/S0304-4203(03)00072-0

different fractions of the DOM pool through the ecosystem. However, due to its complexity, the chemical characterisation of DOM is an arduous process involving large sample volumes and many stages (e.g. Opsahl et al., 1999). As the chemical nature of DOM defines its optical properties, optical measurements have been applied for tracing its variability in natural waters (Kalle, 1966; Coble et al., 1990; Green, 1992; Stedmon and Markager, 2001). The optically active fraction of DOM is called coloured dissolved organic matter (CDOM) and it can be used as a tracer for the dynamics and characteristics of the total DOM pool. As well as absorbing light (being coloured), CDOM also fluoresces when excited by light in the UV and blue region of the spectrum. The two major DOM components that have been found to fluoresce are humic material (a blue fluorescence) and protein fractions (a UV fluorescence) (Mopper and Schultz, 1993; Coble, 1996). Table 1 lists the most common fluorescent peaks seen in each group, identified in natural waters.

Table 1
Positions of the fluorescence maxima of the five components identified by the PARAFAC model

This study			
Component number		Excitation max (nm)	Emission max (nm)
1		<240	436
2		<240	416
3		270 (360)	478
4		325 (250)	416
5		280 (<240)	368
Previously identified			
Label	Description		
	UV humic-like	230	430
A	UV humic-like	260	380–460
C	visible humic-like	320–360	420–460
D	soil fulvic acid	390	509
E	soil fulvic acid	455	521
M	marine humic-like	290–310	370–410
N	associated with phytoplankton productivity	280	370
T	protein-like (tryptophan)	275	340

Wavelengths in brackets represent secondary maxima. Fluorescence peaks identified in earlier work are also shown (Lochmuller and Saavedra, 1986; Coble et al., 1990, 1998; Coble, 1996; Blough and Del Vecchio, 2002).

When a molecule absorbs light (energy), an electron is excited and promoted to an unoccupied orbital. The energy difference between the ground (S_0) and excited singlet states (S_1, S_2 or higher) determines the wavelengths at which light is absorbed. Absorption (excitation) can result in a range of transitions to various vibrational sublevels of excited singlet states. This is the reason that molecular absorption spectra are often seen to consist of broad peaks. Excitation is then followed by nonradiative relaxation to the lowest sublevel of the S_1 state, via vibrational relaxation and internal conversion. Internal conversion, singlet–triplet intersystem crossing and fluorescence then compete for relaxation to the ground state (S_0). The wavelength of the fluorescence emission is determined by the difference in energy between S_1 and S_0 states. The greater the conjugation in the molecule, the lesser the difference in energy, resulting in a longer wavelength of fluorescence.

Fluorescence excitation–emission matrices (EEMs) are the result of merging a series of emission scans from excitations over a range of wavelengths and have previously been used as a tool for the characterisation of CDOM (Coble et al., 1990; Green, 1992; Coble, 1996). This technique provides information on the number and type of fluorophores present as well as their abundance. For example, EEM spectroscopy has been successfully applied to differentiate between CDOM of terrestrial and marine origin (Coble, 1996), marine CDOM having a fluorescence maximum at shorter wavelengths than terrestrial CDOM.

EEMs contain a large amount of information and it is only recently that all this information is being used in studies. Recent work has shown how multivariate data analysis methods (e.g. Principal Component Analysis, PCA) can be applied to the study of EEMs in marine science (Persson and Wedborg, 2001). These methods are relatively fast and allow a more complete data analysis than the traditional ‘‘peak picking’’ techniques. Persson and Wedborg (2001) provide an introduction to multivariate analysis of EEMs using PCA and show how it can be applied to water mass mixing between the Baltic and North Seas. However, it has been argued that two-way PCA models are inadequate for modelling the essentially three-way character of EEMs (Bro, 1997). Each EEM

is in itself a matrix, and by combining EEMs from several samples, a three-way array is obtained (sample by excitation by emission). For PCA analysis, the three-way data have to be unfolded into a two-way matrix with each excitation–emission pair defined as a variable (column) in the matrix. This complicates the modelling and makes the model more difficult to interpret. For example, data measured at 45 different excitation wavelengths and 150 different emission wavelengths would provide a data matrix with $45 \times 150 = 6750$ different variables. Moreover, the result of PCA analysis has an intrinsic *rotational freedom*, which, in essence, means that it is not possible to identify the spectra of the underlying fluorophores from the data.

Parallel factor analysis (PARAFAC), a three-way method with its origin in psychometrics (Harshman, 1970; Caroll and Chang, 1970), is better suited to the complex nature of EEMs. In this application, it can be thought of as a three-way version of PCA, where the data are decomposed into *trilinear* components. Over the past 20 years, a series of studies have shown how PARAFAC can be successfully applied to decompose EEMs of complex mixtures into their individual fluorescent components (Ross et al., 1991; Bro, 1997, 1998, 1999; Jiji et al., 1999; Baunsgaard et al., 2000, 2001; da Silva et al., 2002; among others). Here we apply similar techniques to EEMs of DOM samples taken from Horsens Estuary and its catchment, on the East coast of Denmark. We propose that PARAFAC will become a vital tool aiding the characterisation of the complex DOM pool. This study is part of the European Union DOMAINE project, which is focused on gaining an understanding of quantity, quality, dynamics and effects of DOM exported to and produced in coastal waters.

2. The PARAFAC model

PARAFAC decomposes the data matrix into a set of trilinear terms and a residual array.

$$x_{ijk} = \sum_{f=1}^{F} a_{if} b_{jf} c_{kf} + \varepsilon_{ijk},$$

$$i = 1,\ldots,I; \quad j = 1,\ldots,J; \quad k = 1,\ldots,K \qquad (1)$$

When applying the model to EEMs, x_{ijk} is the intensity of fluorescence for the ith sample at emission wavelength j and excitation wavelength k. a_{if} is directly proportional to the concentration (e.g. moles) of the fth analyte in sample i. b_{jf} is linearly related to the fluorescence quantum efficiency (fraction of absorbed energy emitted as fluorescence) of the fth analyte at emission wavelength j and the matrix $\mathbf{b}_f$ with typical elements b_{jf} is thus an estimate of the emission spectrum of the fth analyte up to a scaling. Likewise, c_{kf} is linearly proportional to the specific absorption coefficient (e.g. molar absorbtivity) at excitation wavelength k. F defines the number of components in the model and a residual matrix ε_{ijk} represents the variability not accounted for by the model. The model is found by the process of minimising the sum of squared residuals. Conversion of the relative concentrations, a_{if}, to actual concentrations either requires knowledge of specific absorption coefficients of each fluorescent component, which a priori is unknown or alternatively requires a calibration based on a known concentration in one or more samples (possibly through standard addition).

How can the estimated PARAFAC components be estimates of the real chemical parameters? The reason is, that unlike PCA, the PARAFAC solutions are uniquely identified up to trivial permutation and scaling without adding mathematical constraints such as orthogonality. This means that they do not suffer from the problem of rotational freedom found in bilinear approaches (e.g. PCA) (Sidiropoulos and Bro, 2000). Hence, in the case that a 'true' trilinear solution provides a best fit to the model, then the model will coincide with the PARAFAC solution. This property of estimating the underlying parameters has been used extensively, for example, in *second-order calibration* (Wang et al., 1993; Booksh and Kowalski, 1994; Ferreira et al., 1995; Bro et al., 1997). As a result, in the case of modelling trilinear EEMs, the estimated loadings spectra will represent the excitation ($\mathbf{c}_f$) and emission ($\mathbf{b}_f$) spectra of the underlying compounds, if the correct number of components is used (Bro, 1999). This ability to extract underlying features from additive mixtures is in stark contrast to virtually all other methods applied for analysing EEM data. The mixtures of signals can be mathematically separated into its constituents much in line with traditional physical chromatographic separations, with no assumptions on spectral shape (except that the different fluorophores

have different spectra), no assumptions on the number of fluorescent components and no statistical assumptions on the structure of noise or the parameters.

An important added advantage of this approach to modelling EEMs is that it is possible to constrain the model parameters. With a general understanding of the data being modelled, certain constraints can be applied to facilitate robust modelling. For example, in the case of modelling fluorescence spectra, one can apply "non-negativity" constraints on the estimates of the concentrations, emission spectra or excitation spectra. This is useful as negative spectra or negative concentrations are not in accordance with the expected nature of the data. Ideally, constraints are not needed for building appropriate models, but model errors can arise, e.g. from scatter effects, and lead to inaccurate estimates. In such cases, added constraints can help to cope with these problems and speed up the modelling process. A more detailed introduction and tutorial to the PARAFAC approach and an example of its applications to modelling fluorescence has recently been published (Bro, 1997, 1999).

3. Methods

The data in this study were collected between the 28th and 30th of August 2001 in the catchment and estuary of Horsens Fjord, located on the East coast of the Jutland peninsula of Denmark. A total of 90 samples were collected, covering all the major terrestrial sources of DOM to streams and the estuary and the mixing of DOM in the estuary with water from the adjacent Kattegat (Fig. 1). DOM samples were filtered through pre-combusted GF/F filters and stored in 100-ml amber glass bottles in the cool and dark. All optical measurements of DOM were made within 2 days. Dissolved organic carbon (DOC) samples were taken in duplicates, filtered through pre-combusted GF/F filters into pre-combusted 10-ml glass tubes and 50-μl 2 N HCl was then added. DOC was measured by the high-temperature combustion method on a Shimadzu TOC-5000 analyser located at the University of Copenhagen, Freshwater Biological Laboratory, using techniques previously described in Søndergaard et al. (2000). DOC concentrations were calculated using a

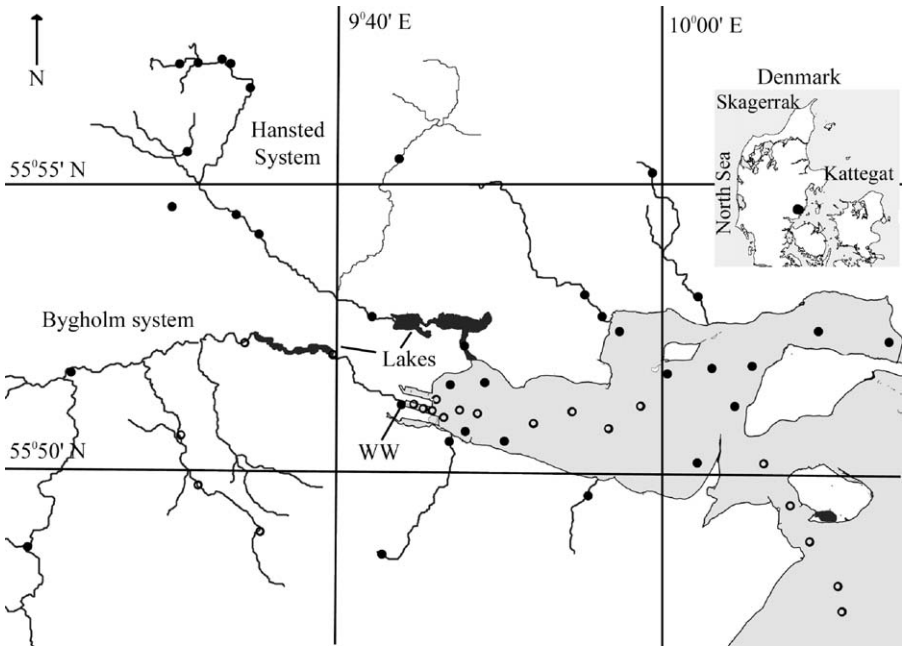

Fig. 1. Map of the Horsens catchment and its location on the east coast of Jutland, Denmark. Filled circles represent sampling stations and hollow circles represent the locations of the samples used in Fig. 7.

four-point calibration curve followed by subtraction of a Milli-Q blank.

Before optical analysis of DOM, the samples were allowed to warm to room temperature. DOM fluorescence measurements were made on a Varian Eclipse fluorescence spectrophotometer. Bandwidths were set to 5 nm for both excitation and emission. A series of emission scans (230–600 nm) were collected over excitation wavelengths ranging from 220 to 450 nm by 5-nm increments. Excitation wavelengths below 240 nm and emission wavelengths below 300 nm were removed due to deteriorating signal to noise ratios.

Fluorescence spectra were corrected for inner filter effects (Mobed et al., 1996). This accounted for the absorption of both excitation and emission light by the sample in the cuvette. This was done according to the methods of McKnight et al. (2001). The spectra (excitation and emission) were also corrected for instrument biases using an excitation correction spectrum derived from a concentrated solution of rhodamine B and an emission correction spectrum derived using a ground quartz diffuser (as recommended by the manufacturer). Comparison of the integrated Raman spectra of Milli-Q water over excitation wavelengths revealed no changes in the lamp intensity during the measurement period. Next, the fluorescence spectra were Raman calibrated by normalising to the area under the Raman scatter peak (excitation wavelength of 350 nm) of a Milli-Q water sample, run the same day. Then a Raman normalised Milli-Q EEM was subtracted from the data to remove the Raman signal. The Raman normalisation and correction procedures resulted in spectra that are in Raman units (R.U., nm^{-1}) and are directly comparable to corrected spectra measured on other machines. The size and shape of the Raman scatter peak are dependent on the instrument optics, setup (bandwidths, PMT voltage, etc.) and lamp age. Normalising the measured signal to the Raman peak and using excitation and emission correction spectra effectively removes all the instrument specific biases. Rayleigh scatter effects were removed from the data set by not including any emission measurements made at wavelengths ≤excitation wavelength +20 nm.

Before modelling, regions of the EMMs that contained limited information (low fluorescence) were removed. This resulted in EEMs that ranged from 240 to 400 and 320 to 580 mm along the excitation and emission axes, respectively. A ‘‘triangle of zeros’’ was also added to the EEMs in the region of missing data (Fig. 2), which corresponds to the region where excitation wavelength is larger than the emission wavelength. This was done partly to speed up the modelling process and also to avoid the model from generating large spurious peaks in this region. The triangle was placed in the region where excitation wavelength was between 355 and 400 nm and emission wavelength was between 320 and 378 nm. The region of zeros was not extended too close to the actual fluorescence data as this would hinder the models’ ability to model fluorescence where emission wavelengths are only slightly larger than excitation wavelengths.

The PARAFAC analysis was performed in MATLAB using the ‘‘N-way toolbox for MATLAB ver. 2.0’’ (Andersson and Bro, 2002) using default numerical settings. The model was run with nonnegativity constraints applied to each dimension. Initially, simple two- to three-component models were run in order to identify outliers in the data set. Four samples (two samples of wastewater and two samples from forest streams) were removed from the data set as outliers. A series of PARAFAC models with one to six components were fitted to the data. In order to avoid the model from converging in local minima (i.e. algorithm converging not at the least squares solution) and to speed up the modelling process, initialisation values were derived from singular value decomposition (SVD; similar to Principle Component Analysis) vectors. Comparing the similarity of the fit with models initialised with random values served to further verify that a local minimum solution was not obtained. Determination of the appropriate rank (number of components) of the model was done by split-half analysis and analysis of residuals and loadings (Harshman and Lundy, 1984).

Split-half analysis involves dividing the data set into two random, typically equal sized groups and, consequently, making a PARAFAC model on both halves independently. If the correct number of components is chosen, the loadings from both the models will be the same, due to the uniqueness of the PARAFAC model (Bro, 1997, 1998; Sidiropoulos and Bro, 2000). Validation using this technique also minimises the likelihood of arriving at a local minimum, as two models with completely different data (the two halves) have

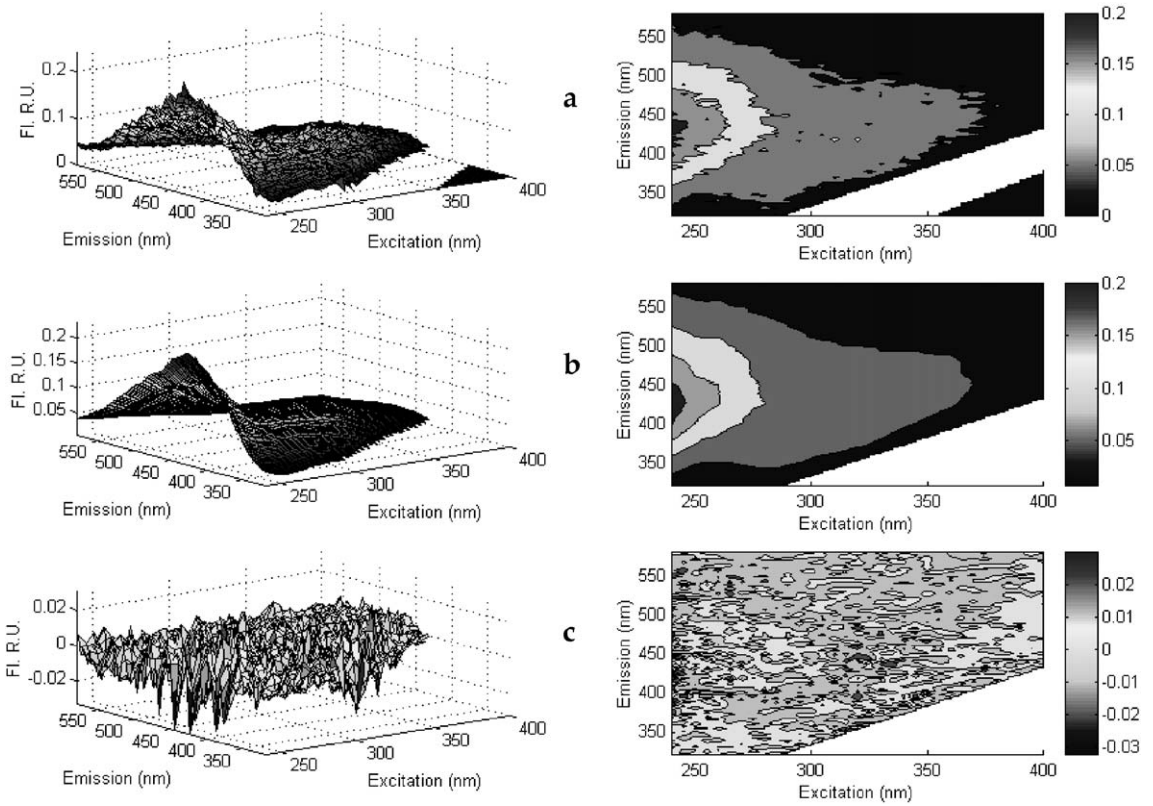

Fig. 2. Example surface and contour graphs of a measured EEM and modelling results for a typical mid estuarine sample: (a) measured, (b) modelled and (c) residual EEM (note: change in *z*-axis scale). Represents a sample with low signal to noise ratio. Fluorescence is shown in Raman units (R.U., nm^{-1}).

arrived at essentially the same solution. It was found that with this data set, up to five components could be validated this way. The best degree of overlap was seen in the emission loadings. This most likely reflects the fact that the emission spectra were better resolved (measured every 2 nm) than the excitation spectra (every 5 nm). Fig. 3 shows the overlapping excitation and emission loadings from five-component models on the two halves of the data set and the whole data set. Scientifically, such a close similarity provides strong empirical evidence that the model is not reflecting random noise in the data but rather intrinsic variation found in two independent data sets (Harshman and Lundy, 1984). Comparison of the sum of squared differences between the split-half excitation and emission loadings for each component in four-, five- and six-component models also revealed a considerable decrease in the overlapping of component loadings for the six-component model. The ranges of sum of squares for each model where 0.001–0.09, 0.003–0.08 and 0.002–1.3, for the four-, five- and six-component models, respectively, relating to a 14-fold increase difference when applying a model with more than five components.

In common with bilinear models, the fit of PARAFAC models can also be assessed by residual analysis. The presence of systematic variations in the residual spectra might suggest that more components can be extracted (although non-trilinear variation, e.g. due to scatter should remain in the residuals). As up to five components could be validated by the split-half analysis, the residuals from four- and five-component models were compared. It was evident that the residuals from the four-component model contained a considerable amount of systematic variation in all samples, whereas the five-component models fitted

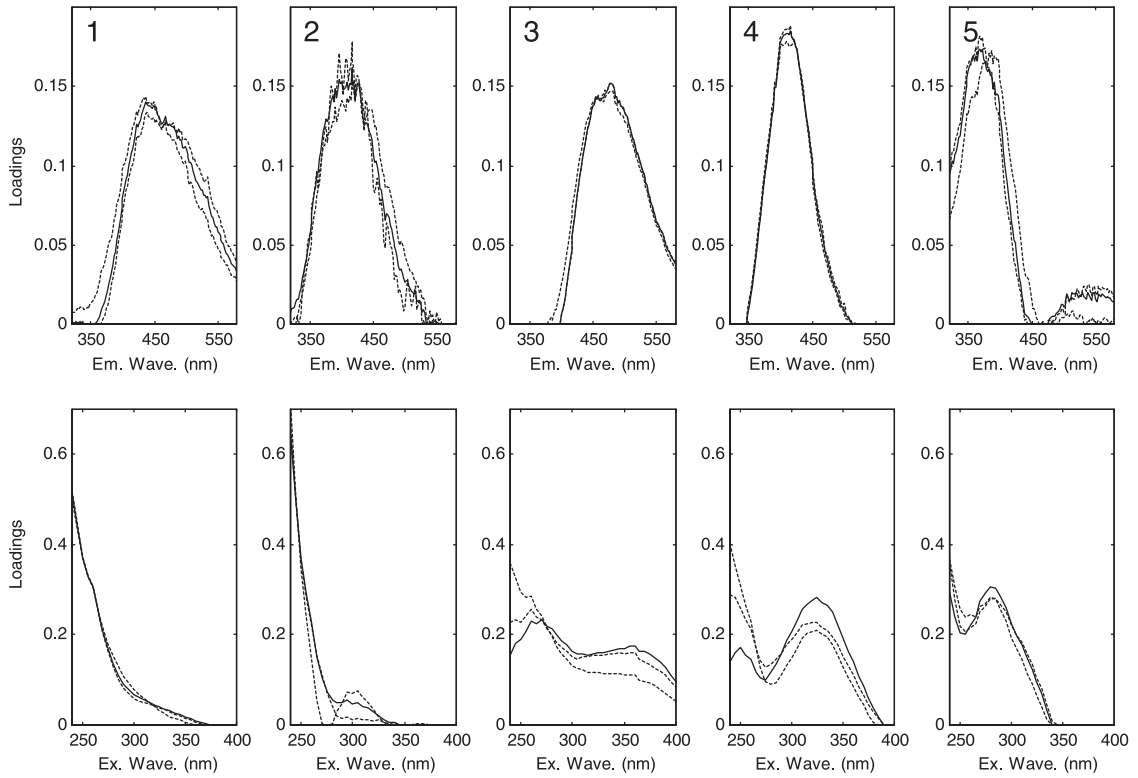

Fig. 3. Excitation and emission loadings produced from two independent, five-component PARAFAC models on two random halves of the complete data set. The high degree of similarity validates the five-component model (dashed lines). The solid line represents the loadings from the five-component model derived using the whole data set.

the measured EEMs better. Fig. 2 shows an example of the residual EEM for a sample collected at a mid-fjord station. One can see that the residuals contain limited systematic deviations. The reasons why PARAFAC cannot be expected to give pure random noise in the residuals are the difficulty in distinguishing weak fluorescing components from instrument noise, minor quenching effects, remaining inner filter effects and scattering effects. However, the results from the split-half analysis and residual analysis allow us to conclude that a five-component model is proper for the data. This is not to say that the EEMs only contained five different fluorophore groups, but rather that these five fluorescent groups where present in the majority of these samples, could be modelled (and validated) by the trilinear model and could explain most of the variation. Other fluorescent groups are certainly present, but their influence is so weak that they cannot be distinguished from the noise.

4. Results and discussion

The variability explained by the model was high and ranged from 96.6% to 99.9%, which is much higher than that possible by other techniques tried by the authors (e.g. nonlinear regressions of 3-D gauss curves). The lowest values were for the marine samples and this was due to the lower DOM concentrations and consequent lower signal to noise ratios in the measurements. An example of measured, modelled and residual EEMs can be seen in Fig. 2. The figure shows that the model reproduces all the main features of the measured EEMs. Fig. 4 shows the integrated emission intensity at each excitation wavelength, for the modelled and measured spectra for an example freshwater and saline sample. Although there are small deviations, it is clear that the model fits the measured data well.

Fig. 5 shows contour plots of each component identified by a five-component PARAFAC model.

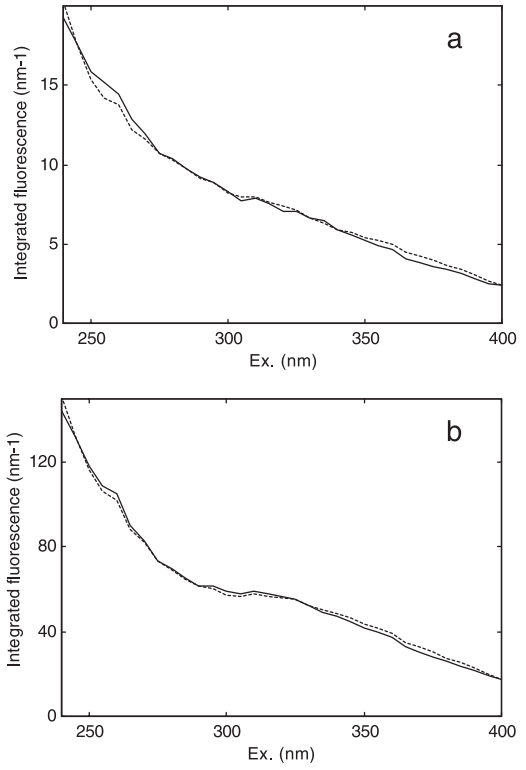

Fig. 4. The integrated emission intensity over excitation wavelength for: (a) a sample taken from the surface waters of the outer estuary and (b) a sample taken from the outflow from Bygholm lake (refer to Fig. 1). Solid line represents the measured data and the dashed line, the modelled data.

They represent five different components that are present in the data set; however, all five are not necessarily present in all samples. The positions of the fluorescence maxima are reported in Table 1 along with the positions of fluorescence maxima identified in earlier studies. The components represent different groups of fluorophores present, exhibiting rounded peaks, multiple excitation maxima and single emission maxima, as often seen in organic fluorophores. The fact that the components have unimodal emission maxima suggests that the model was successful at grouping the fluorophores present into groups with similar fluorescence/molecular structure, even though the model was not constrained to do this. The existence of multiple emission bands within a component would imply the presence of greatly differing fluorophores.

The peaks identified in this study show many features in common with previously identified peaks (Coble et al., 1990, 1998; Coble, 1996; Blough and Del Vecchio, 2002) and differences are most likely due to uncertainties arising from the interpretation of the spectra using traditional "peak picking" techniques. Components 1, 3 and 4 are similar to peaks previously associated with UV humic-like material (Table 1). Component 1 absorbs only in the UVC-region and its maximum absorption is below 240 nm, the lower limit of the measurements in this study. The emission peak is very broad with maximum at 436 nm (Figs. 3 and 5). Both features correspond to peak A in the literature. Peak A fluorescence has been observed in both marine and terrestrial CDOM (Coble et al., 1990, 1998; Coble, 1996; De Souza Sierra et al., 1994). In this study it is found to dominate the EEMs of CDOM from forested and wetlands regions. Component 2 exhibits a similar excitation spectrum to component 1 but has a blue shifted emission. It is not similar to any of the previously identified peaks. Component 3 exhibits both UVC and UVA excitation maxima and an emission peak centred at 478 nm. Its characteristics are similar to that of peak C from the literature, which is thought to represent humic material exported from terrestrial sources (Coble et al., 1998). A recent degradation study also suggested the existence of such a fluorophore (Boehme and Coble, 2000). Component 4 also shows a double excitation maxima and a single, well-defined emission peak at 416 nm. It could be similar to peak M (Table 1) although it differs in excitation characteristics. Moreover, peak M is thought to represent marine humic matter (Coble et al., 1998), but the appearance of component 4 in our terrestrially dominated end-member samples (Fig. 6) shows that, in this study, it is most likely a peak originating from terrestrially derived organic matter. Component 5 also shows two excitation maxima, one at 280 nm and another at wavelengths below 240 nm. This component is very similar to N in Table 1, however, could be a combination of peaks N and T. Peak N is believed to represent labile material produced as a result of biological production in the water column (Coble et al., 1998). Peak T has fluorescence properties similar to the indole ring structure of tryptophan and this protein fluorescence has also been associated with biological production in surface waters (Coble et al., 1998; Determann et al., 1994; Determann et al., 1996). It is possible that with a larger data set, this

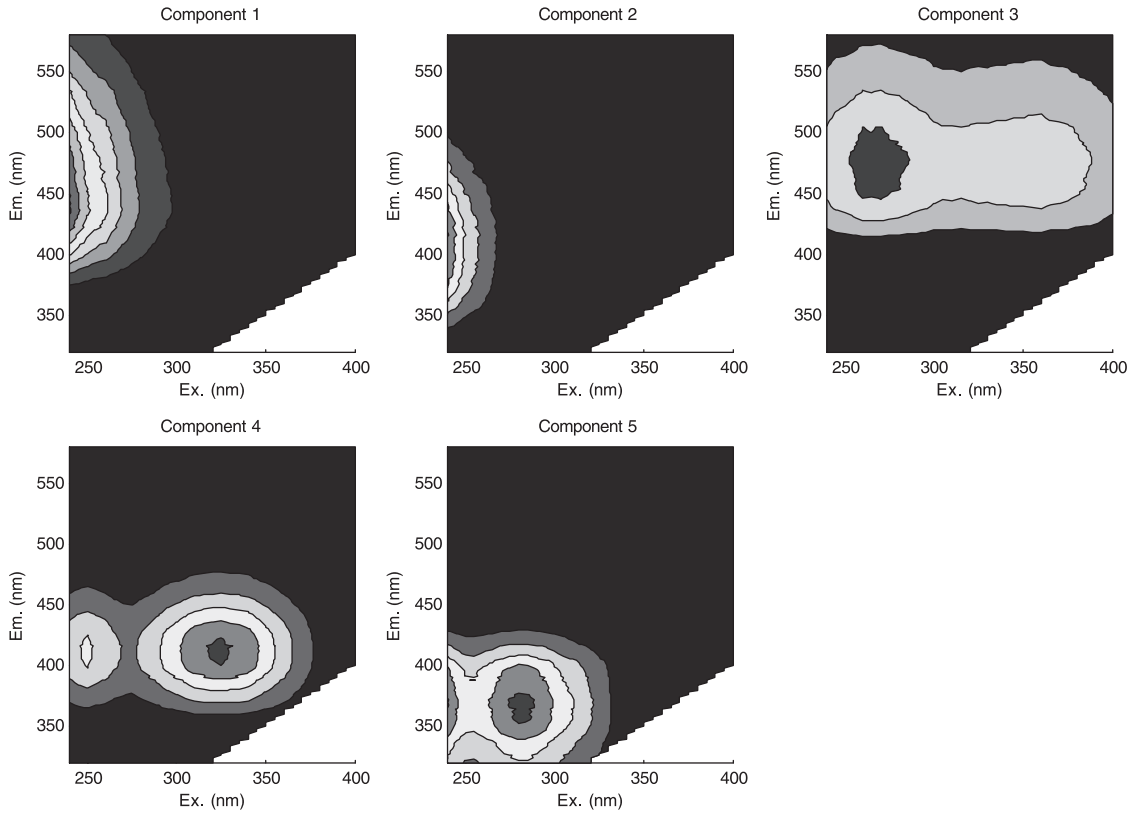

Fig. 5. The five different fluorescent components found by the PARAFAC model. Refer to Table 1 for the positions of their maxima.

component could have been resolved into the two different peaks; however, with the present data set, this could not be validated.

The fact that components 1 and 3 exhibit emission at longer wavelengths than the other components suggests that they contain more conjugated fluorescent molecules than the other components (Sharma and Schulman, 1999). Excitation at longer wavelength suggests that the fluorophores responsible for this fluorescence are more aromatic in nature or contain several functional groups (Coble et al., 1998). It is likely that component 3 represents a high molecular weight fraction of the terrestrially derived humic matter. This is supported by the results from recent work that found that the ratio of fluorescence in this region (~ 500 nm) relative to the fluorescence at 450 nm, varies depending on the number of aromatic groups and, hence, the source of the material (McKnight et al., 2001).

The differences in the position of the excitation and emission maxima between the results of this study and previous work are most likely due to the different approaches to peak identification applied. For example, if the fluorescence spectra of components 3 and 4 are summed, we observe excitation maxima at 260 and 325 nm and an emission maximum at 430 nm, which is very similar with the positions of reported A and C maxima (Coble, 1996). The overlapping of absorption bands leads to the displacement of maxima from true maxima and can therefore hinder the visual localisation of different fluorescence maxima in a complex mixture. The approach used here does not suffer from this disadvantage. However, our approach does have its own limitations. The number of components identified by the model depends to a certain extent on the degree of variability in the concentrations of each component and their independent behaviour. For example, if two groups were highly correlated in their

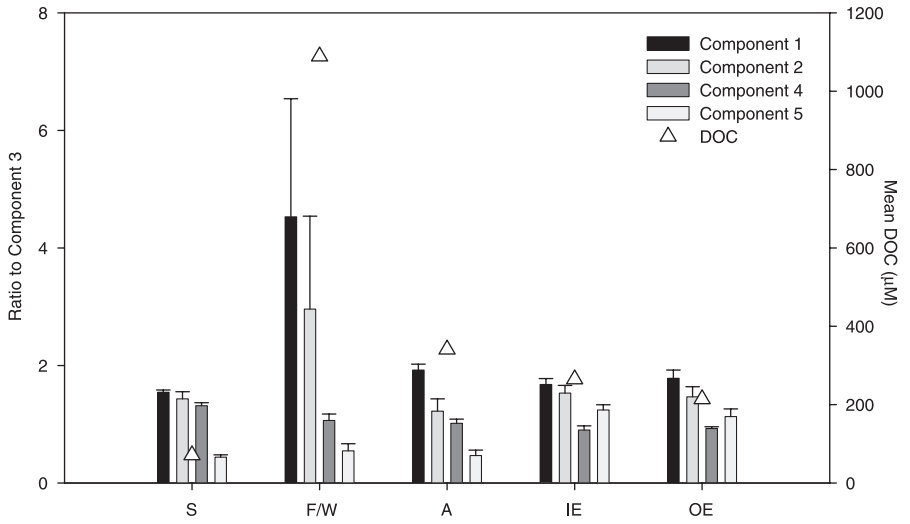

Fig. 6. Characterisation of the different DOM end-members in the Horsens catchment. The chart shows the mean ratios of each component fluorescence maximum to the fluorescence maximum of component 3 and the mean DOC concentration for each group of samples. S indicates spring water samples ($n=2$) taken at stations located at the source of streams. F/W represents samples taken in forest streams and wetlands ($n=8$). A indicates samples taking in streams draining agricultural areas ($n=5$). IE and OE represent inner and outer estuary stations ($n=14$ and 9, respectively). Error bars represent one standard deviation.

appearance among samples and/or had very similar fluorescence characteristics, the model would have difficulty in separating the two. This is possibly the case for component 5 as mentioned earlier. In order to circumvent this, it is best to apply PARAFAC to large data sets. Another area where care is needed when applying PARAFAC, is in the selection of a data set. The components derived by the model have fixed excitation and emission characteristics and the model is not capable of allowing small shifts in maxima between samples. Shifts can occur as a result of changes in the solvent properties (e.g. pH and salinity). However, as mentioned earlier, it is also likely that some of the shifts in maxima reported in the literature are purely due to the presence or absence of one of several overlapping components.

Fig. 6 shows the differences in composition of the EEMs between the different Horsens catchment end-members sampled. The data are averages for the different types of CDOM sampled. The data are shown as ratios to component 3 (peak C), as this component is thought to represent a terrestrially derived component that has been found to be present in a wide range of environments (Coble, 1996). Presented in this way, the data reflect the differences in composition rather than the considerable differences in concentration (as can be seen in the DOC data on the same figure). For all the components except component 4, the ratios varied considerably between the different end-members, indicating that the components were independently variable. Component 4 showed only slight differences between end-members, suggesting that it behaved similarly to component 3 (C.V. 55%, 41%, 16% and 51% for the ratios of components 1, 2, 4 and 5, respectively). Components 1 and 2 were characteristic of the forest stream and wetland water EEMs. Component 5 ratios were twice as large in the estuary than in the terrestrial samples, suggesting that the fluorescence in this component is not only due to terrestrially derived matter but also CDOM produced/transformed in estuarine processes. The small differences observed between the inner and outer estuarine samples suggests that there are no noticeable changes occurring to the CDOM composition during its transport within the estuary. This is most likely due to the low freshwater input to the estuary during the summer months, resulting in the majority of DOM imported to the estuary coming from the bordering coastal waters. Although having considerably lower DOC concentrations and CDOM fluorescence, the spring water CDOM had a very similar composition of components 2–5 as the agricultural CDOM had, suggesting that it probably

consisted of some agricultural runoff diluted with pure groundwater. The results in Fig. 6 show that this technique is capable of distinguishing between CDOM derived from different sources. For example, there are considerable differences in the composition of CDOM from the two major sources of DOM in the catchment, forest/wetlands and agricultural areas.

Fig. 7 shows the compositional changes in the CDOM pool down one of the two major stream systems supplying the estuary and in the estuary itself. As CDOM is transported through the system, major decreases in its fluorescence intensity occur. These occur as CDOM is transported out of the forest and again during estuarine mixing. The fall in fluorescence intensities observed in the freshwater environment cannot be explained by mixing (dilution) alone and therefore also represents degradation or transformations occurring as the DOM pool is transported downstream. As the forest stream is mostly shaded from exposure to direct sunlight, it is likely that part of the initial fall in fluorescence intensity and DOC concentration is due to photochemical degradation processes

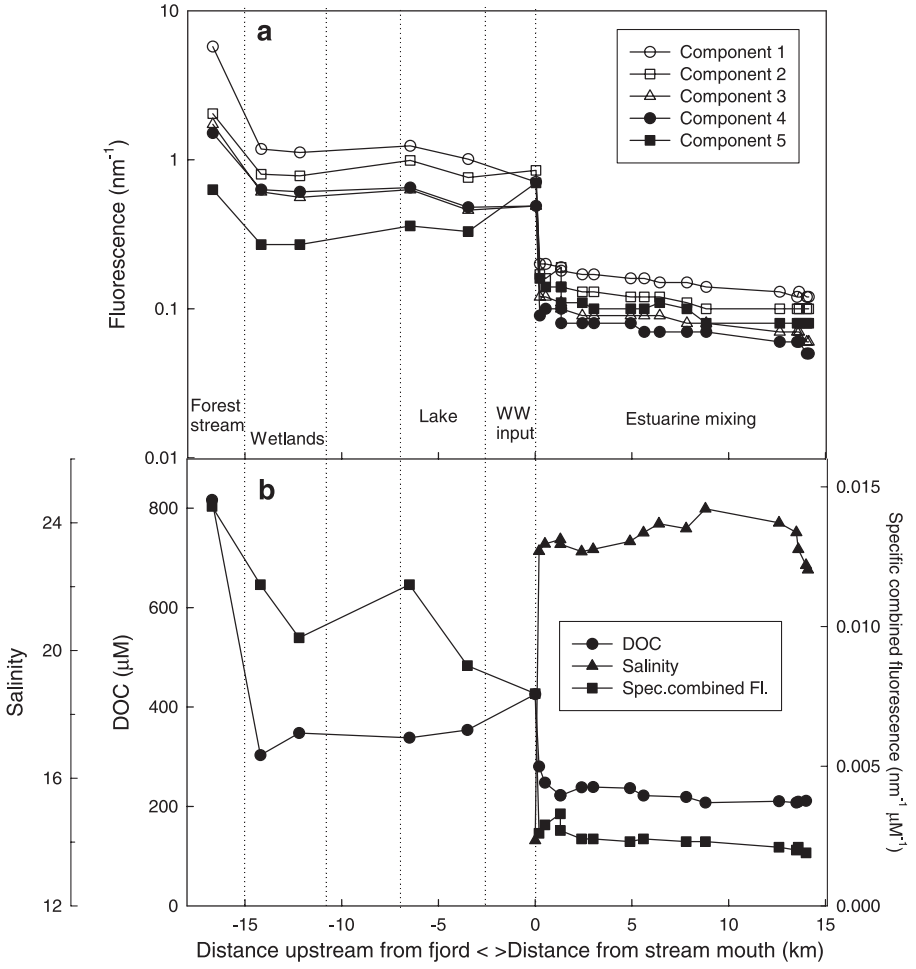

Fig. 7. (a) The behaviour of the CDOM pool and changes in its composition down one of the two major stream systems supplying freshwater to Horsens Fjord (Bygholm Å). The first station was located in a forest stream. The water passed through a wetlands region and a lake, before mixing with the saline fjord water. In the mixing zone, there was a point source input of DOM from the town's wastewater treatment plant. (b) The behaviour of DOC, salinity and DOC-specific combined fluorescence (sum of peak fluorescence values of each component divided by the DOC concentration) through the system.

taking place in the streams as it is transported out of the forest and through the wetlands. This is supported by the concurrent decline in specific fluorescence values seen (Fig. 7b). Photochemical degradation bleaches the DOM fluorescence and causes the specific fluorescence to decrease (Vodacek et al., 1995). This is also the case for the changes seen during passage through the lake, where the water has a longer residence time and hence greater exposure to surface light. The overall increase in DOC concentrations during passage through the lake suggests that there is also a net production of autochthonous DOM in the lake. This is in accordance with the high chlorophyll levels measured in the waters draining the lake (115μg/l) and the fact that the fluorescence component 5, which is known to be associated with phytoplankton activity (Coble et al., 1998), did not decrease to the same extent as the other components (10% compared to 19–28%).

The second major decrease in CDOM fluorescence and DOC concentrations is seen during estuarine mixing where the freshwater input from the stream mixes with the saline waters of the inner estuary. There is also a wastewater discharge from Horsens town, located in the mixing zone. Due to the low flow conditions during summer, this mixing zone was very constrained and lay in the stream itself. Stream water accounted for ~ 70% and wastewater ~ 30% of the freshwater input from the Bygholm system into the estuary. The first saline station sampled (0 km, salinity = 14.03) had a higher DOC concentration due to the additional input from the wastewater plant. The effect of the wastewater plant discharge can also be seen in the increased fluorescence of component 5. Although the wastewater EEMs where not included in this PARAFAC model, a recent study has shown that wastewater CDOM has a considerable fluorescence in the same spectral region as component 5 (Baker, 2001). As seen earlier in Fig. 6, the composition of the CDOM fraction did not undergo any noticeable changes during its transport through the estuary, due to the well-mixed nature of the estuary during summer (Fig. 7). The salinity measurements revealed that all but one of the estuarine samples taken had a salinity between 22.53 and 24.44. The reason for the slight fall in salinity outside the mouth of the estuary is due to the fluctuating salinity of the coastal waters outside the estuary, which are part of the Kattegat (Baltic Sea–North Sea mixing zone).

Considering the fluorescence characteristics, behaviour in the catchment and similarity to previously identified fluorescent peaks, it can be concluded that the five different components can be generally grouped into three different types of fluorescent organic matter. (1) The UVC humic-like components 1 and 2, which dominate the EEMs of terrestrially derived organic matter end-members. (2) The UVA humic-like components 3 and 4, which are present in similar proportions over a range of different environments and also appear to be derived from the degradation of terrestrial organic matter. (3) A UVB excitable component with a UVA fluorescence, which, although also containing a terrestrial organic matter signal, includes a fraction of autochthonous DOM.

5. Conclusions

The agreement between the model components and previously identified peaks is encouraging and suggests that PARAFAC modelling is an effective method of characterising CDOM with EEMs. By using the appropriate model rank, different fluorophore groups present in the matrices can be identified. Previously, this was not possible. This modelling approach permits the tracing of some of the different fractions of the DOM pool in aquatic ecosystems and will facilitate our understanding of the processes governing DOMs concentration and its characteristics. Further study of the behaviour and distributions of each fluorescent component could also enable us to establish relationships between general characteristics of the DOM pool and its fluorescent properties (e.g. bioavailability, nitrogen and phosphorous content). Land use in river catchment and coastal regions influences the quantity and quality of DOM exported to rivers, lakes and coastal waters. This technique allows an assessment of the impact of land use on DOM export to adjacent aquatic ecosystems, thereby providing a useful tool in catchment management.

Acknowledgements

This work was supported by the European Union 5th framework DOMAINE project (EVK 3-CT-2000-00034) and the Danish Research Agency no. 641-00-

0006. The authors would like to thank Niels Henrik Borch for providing the DOC data and the Danish participants of the DOMAINE project for their help in sampling. CS would also like to thank P. Coble, J. Boehme and R. Conmy for invaluable discussions of the subject area. Finally, we would like to thank Morten Søndergaard and two anonymous reviewers for their comments on the manuscript (ELOISE no. 372/42).

Associate editor: Dr. Edward Peltzer.

Appendix A. Description of data used

Sample type	Location	Station	Date	Depth (m)	Salinity	Chl-*a* (μg/l)	DOC (μM)	R^2	F_{max} 1	F_{max} 2	F_{max} 3	F_{max} 4	F_{max} 5
Estuarine	Inner estuary	3	28-Aug-01	1		19.4	237	0.977	0.169	0.121	0.093	0.077	0.105
	Inner estuary	3	28-Aug-01	3		20.0	234	0.979	0.166	0.127	0.093	0.078	0.103
	Inner estuary	3	30-Aug-01	1		9.2	234	0.973	0.154	0.120	0.084	0.072	0.103
	Inner estuary	3	30-Aug-01	3		8.4	231	0.976	0.155	0.122	0.087	0.074	0.102
	Inner estuary	4	28-Aug-01	1	23.1	10.7	242	0.977	0.176	0.128	0.097	0.080	0.112
	Inner estuary	4	30-Aug-01	1	18.1	13.4		0.977	0.170	0.131	0.094	0.078	0.112
	Inner estuary	5	28-Aug-01	1	22.0	16.5	265	0.982	0.264	0.248	0.156	0.144	0.182
	Inner estuary	5	30-Aug-01	1	23.1	24.0	280	0.970	0.202	0.169	0.117	0.089	0.160
	Inner estuary	101	28-Aug-01	1	23.6	9.2	257	0.970	0.203	0.251	0.129	0.109	0.167
	Inner estuary	102	28-Aug-01	1	23.5	12.5	223	0.976	0.187	0.193	0.114	0.097	0.139
	Inner estuary	103	28-Aug-01	1	23.3	16.4	222	0.979	0.176	0.142	0.096	0.082	0.111
	Inner estuary	104	28-Aug-01	1	23.1	12.8	239	0.978	0.168	0.132	0.093	0.077	0.106
	Inner estuary	105	28-Aug-01	1	23.2	15.7	239	0.978	0.169	0.132	0.094	0.079	0.103
	Inner estuary	106	28-Aug-01	1	23.4	12.9	237	0.978	0.159	0.123	0.089	0.076	0.097
	Inner estuary	107	28-Aug-01	1	23.7	12.4	222	0.976	0.156	0.115	0.086	0.073	0.096
	Inner estuary	108	28-Aug-01	1	24.0	12.2		0.974	0.153	0.118	0.085	0.071	0.109
	Inner estuary	109	28-Aug-01	1	23.8	9.3	219	0.975	0.150	0.107	0.081	0.067	0.098
	Inner estuary	110	28-Aug-01	1	24.4	6.2	208	0.977	0.138	0.105	0.077	0.068	0.084
	Inner estuary	121	28-Aug-01		18.1	18.4	292	0.988	0.435	0.413	0.253	0.258	0.284
	Inner estuary	121	30-Aug-01		14.1	29.1	426	0.966	0.705	0.852	0.492	0.486	0.696
	Inner estuary	122	28-Aug-01		23.7	17.9	242	0.975	0.200	0.192	0.121	0.101	0.153
	Inner estuary	122	30-Aug-01		23.3	20.0	248	0.976	0.201	0.162	0.116	0.099	0.143
	Inner estuary	123	28-Aug-01		22.7	5.9	267	0.981	0.237	0.200	0.134	0.117	0.158
	Inner estuary	124	28-Aug-01		23.5	14.2	241	0.979	0.173	0.126	0.095	0.078	0.110
	Inner estuary	125	30-Aug-01		23.4	3.3	257	0.978	0.210	0.165	0.120	0.099	0.133
	Inner estuary	126	30-Aug-01		23.4	4.7	255	0.977	0.194	0.167	0.114	0.095	0.137
	Middle estuary	2	28-Aug-01	15		3.7	149	0.975	0.100	0.078	0.063	0.060	0.060
	Middle estuary	2	28-Aug-01	1		11.0	231	0.977	0.156	0.120	0.086	0.072	0.095
	Middle estuary	2	30-Aug-01			4.9		0.978	0.139	0.112	0.081	0.071	0.089
	Middle estuary	2	30-Aug-01	1		7.2	216	0.976	0.139	0.108	0.071	0.060	0.088
	Middle estuary	111	28-Aug-01	1	23.8	10.5	225	0.978	0.153	0.118	0.086	0.072	0.094
	Middle estuary	112	28-Aug-01	1	23.1	11.8	260	0.980	0.183	0.121	0.100	0.081	0.105
	Middle estuary	113	28-Aug-01	1	23.4	10.2	229	0.977	0.153	0.113	0.084	0.072	0.094
	Middle estuary	114	28-Aug-01	1	23.7	8.9	230	0.980	0.160	0.123	0.088	0.076	0.096
	Middle estuary	115	28-Aug-01	1	24	7.1	210	0.978	0.130	0.103	0.073	0.063	0.080
	Middle estuary	116	28-Aug-01	1	23.7	5.9	208	0.973	0.120	0.098	0.066	0.059	0.079
	Middle estuary	117	28-Aug-01	1	23.2	4.7	209	0.974	0.125	0.101	0.066	0.060	0.085
	Middle estuary	127	30-Aug-01		25.0	3.5	207	0.972	0.137	0.103	0.078	0.066	0.098
	Middle estuary	128	30-Aug-01		23.0	3.3	224	0.976	0.141	0.111	0.075	0.064	0.093
	Middle estuary	129	30-Aug-01		23.7	4.2	239	0.966	0.152	0.111	0.087	0.067	0.119
	Middle estuary	130	30-Aug-01		23.6	5.4	261	0.977	0.179	0.125	0.099	0.080	0.118
	Middle estuary	131	30-Aug-01		22.2	6.4	269	0.978	0.188	0.141	0.100	0.078	0.119
	Middle estuary	132	30-Aug-01		23.1	4.3	276	0.978	0.221	0.139	0.119	0.090	0.138

(continued on next page)

Appendix A (*continued*)

Sample type	Location	Station	Date	Depth (m)	Salinity	Chl-*a* (μg/l)	DOC (μM)	R^2	F_{max} 1	F_{max} 2	F_{max} 3	F_{max} 4	F_{max} 5
Estuarine	Middle estuary	133	30-Aug-01		23.4	5.1	266	0.976	0.196	0.147	0.104	0.079	0.133
	Middle estuary	134	30-Aug-01		24.7	2.3	263	0.976	0.186	0.115	0.104	0.078	0.116
	Middle estuary	135	30-Aug-01		22.6	6.5	234	0.973	0.183	0.130	0.100	0.080	0.120
	Middle estuary	200	30-Aug-01			12.3	342	0.979	0.176	0.135	0.097	0.084	0.113
	Middle estuary	201	30-Aug-01			12.9	259	0.978	0.176	0.128	0.093	0.079	0.114
	Middle estuary	202	30-Aug-01			26.9	344	0.980	0.231	0.179	0.128	0.110	0.146
	Outer estuary	1	28-Aug-01	8.5		5.9	186	0.975	0.117	0.093	0.070	0.064	0.075
	Outer estuary	1	28-Aug-01	5		4.2	232	0.974	0.123	0.104	0.064	0.057	0.081
	Outer estuary	1	28-Aug-01	16.5		4.5		0.975	0.099	0.073	0.062	0.058	0.057
	Outer estuary	1	30-Aug-01			3.9	224	0.977	0.140	0.110	0.075	0.068	0.090
	Outer estuary	1	30-Aug-01	1		3.4		0.982	0.193	0.171	0.113	0.111	0.115
	Outer estuary	1	30-Aug-01	5		6.0	216	0.976	0.145	0.118	0.078	0.073	0.095
	Outer estuary	1	30-Aug-01	16.5		4.6		0.973	0.114	0.090	0.070	0.066	0.071
	Outer estuary	118	28-Aug-01	1	22.7	4.4	211	0.975	0.118	0.099	0.061	0.055	0.077
	Outer estuary	119	28-Aug-01	1	22.5	4.3		0.975	0.116	0.101	0.061	0.053	0.078
Freshwater	Forest stream	26	29-Aug-01			5.3	816	0.999	5.749	2.038	1.729	1.506	0.631
(Bygholm system)	Inflow to aquaculture plant	33	29-Aug-01			24.5	398	0.998	1.470	1.222	0.704	0.737	0.389
	Outflow from aquaculture plant	34	29-Aug-01			25.9	450	0.998	1.464	1.338	0.714	0.733	0.467
	Inflow to wetlands	24	29-Aug-01			16.0	303	0.997	1.183	0.802	0.609	0.635	0.270
	Outflow from wetlands	23	29-Aug-01			13.4	348	0.997	1.116	0.785	0.564	0.609	0.271
	Lake inflow	6	29-Aug-01			2.9	338	0.997	1.245	0.990	0.630	0.653	0.365
	Lake outflow	7	29-Aug-01			114.8	354	0.995	1.007	0.759	0.456	0.483	0.328
Freshwater	Forest stream	54	29-Aug-01			2.8	1051	0.999	9.015	2.991	2.305	1.902	0.933
(Hansted	Forest stream	46	29-Aug-01			1.4	274	0.995	0.658	0.436	0.358	0.371	0.136
system)	Inflow to aquaculture plant	31	29-Aug-01			3.1	369	0.997	1.342	0.895	0.642	0.623	0.328
	Outflow from aquaculture plant	32	29-Aug-01			2.5	428	0.998	1.411	1.039	0.661	0.663	0.379
	Lake inflow	8	29-Aug-01			7.7	521	0.998	3.007	1.642	1.054	1.096	0.462
	Lake outflow	9	29-Aug-01			48.4	569	0.996	2.314	1.414	0.776	0.811	0.525
	Outflow from wetlands	14	29-Aug-01			1.3	459	0.997	1.775	1.049	0.761	0.801	0.303
	Wetlands region	45	29-Aug-01			4.5	841	0.999	4.910	2.802	1.478	1.511	0.756
	Wetlands region	53	29-Aug-01			38.2	293	1.000	20.04	14.35	2.606	2.958	1.730
	Wetlands region	55	29-Aug-01			1.9	251	0.999	13.55	10.94	2.853	3.479	1.926
Freshwater	Drainage of clay soils	38	29-Aug-01			3.0	169	0.995	0.456	0.347	0.293	0.316	0.130
(others)	Drainage of clay soils	52	29-Aug-01			1.2	342	0.996	1.888	0.721	0.784	0.685	0.281
	Spring water	50	29-Aug-01			0.2	67	0.991	0.220	0.189	0.140	0.180	0.057
	Spring water	51	29-Aug-01			0.3	76	0.990	0.227	0.226	0.149	0.201	0.070
	Stream with primarily agricultural catchment	10	29-Aug-01			11.7	312	0.996	1.127	0.927	0.640	0.705	0.378
	Stream with primarily agricultural catchment	11	29-Aug-01			2.0	305	0.997	1.240	0.764	0.632	0.633	0.287
	Stream with primarily agricultural catchment	12	29-Aug-01			9.5	305	0.997	1.196	0.667	0.595	0.565	0.270
	Stream with primarily agricultural catchment	28	29-Aug-01			2.5	381	0.997	1.193	0.914	0.634	0.695	0.340
	Stream with primarily agricultural catchment	29	29-Aug-01			2.7	403	0.997	1.701	0.831	0.859	0.818	0.299
	Urban drain	35	29-Aug-01			0.8	347	0.996	1.420	0.947	0.684	0.726	0.260
	Urban drain	36	29-Aug-01				617	0.995	2.319	1.980	0.994	1.426	0.457

F_{max} refers to the fluorescence intensity in Raman units (nm^{-1}) at the fluorescence maximum stated in Table 1.

References

Andersson, C.A., Bro, R., 2002. The N-way toolbox for MATLAB. Chemom. Intell. Lab. Syst. 52, 1–4 (Toolbox available at http://www.models.kvl.dk/source/).

Baker, A., 2001. Fluorescence excitation–emission matrix characterisation of some sewage impacted rivers. Environ. Sci. Technol. 35, 948–953.

Baunsgaard, D., Munck, L., Nørgaard, L., 2000. Evaluation of the quality of solid sugar samples by fluorescence spectroscopy and chemometrics. Appl. Spectrosc. 54 (3), 438–444.

Baunsgaard, D., Nørgaard, L., Godshall, M.A., 2001. Specific screening for color precursors and colorants in beet and cane sugar liquors in relation to model colorants using spectrofluorometry evaluated by HPLC and multiway data analysis. J. Agric. Food Chem. 49 (4), 1687–1694.

Berault, R.F., Colman, J.A., Aiken, G.R., McKnight, D.M., 1996. Copper speciation and binding by organic matter in stream water. Environ. Sci. Technol. 30, 3477–3486.

Blough, N.V., Del Vecchio, R., 2002. Chromophoric DOM in the coastal environment. In: Hansell, D.A., Carlson, C.A. (Eds.), Biogeochemistry of Marine Dissolved Organic Matter. Academic Press, Elsevier, p. 509. Imprint.

Boehme, J.R., Coble, P.G., 2000. Characterization of colored dissolved organic matter using high-energy laser fragmentation. Environ. Sci. Technol. 34, 3283–3290.

Booksh, K.S., Kowalski, B.R., 1994. Theory of analytical chemistry. Anal. Chem. 66, 782A–791A.

Bricaud, A., Morel, A., Prieur, L., 1981. Absorption by dissolved organic matter of the sea (yellow substance) in the UV and visible domains. Limnol. Oceanogr. 26, 43–53.

Bro, R., 1997. PARAFAC. Tutorial and applications. Chemom. Intell. Lab. Syst. 38, 149–171.

Bro, R., 1998. Multi-way analysis in the food industry. Models, algorithms, and applications. PhD thesis. University of Amsterdam, Netherlands.

Bro, R., 1999. Exploratory study of sugar production using fluorescence spectroscopy and multi-way analysis. Chemom. Intell. Lab. Syst. 46, 133–147.

Bro, R., Workman Jr., J., Mobley, P., Kowalski, B.R., 1997. Review of chemometrics applied to spectroscopy: 1985–1995, Part III. Multi-way analysis. Appl. Spectrosc. Rev. 32, 237–261.

Carlson, C., 2002. Production and removal processes. In: Hansell, D.A., Carlson, C.A. (Eds.), Biogeochemistry of Marine Dissolved Organic Matter. Academic Press, Elsevier, p. 91. Imprint.

Caroll, J.D., Chang, J., 1970. Analysis of individual differences in multidimensional scaling via an N-way generalisation of and Eckart–Young decomposition. Psychometrika 35, 283.

Coble, P.G., 1996. Characterisation of marine and terrestrial DOM in seawater using excitation–emission matrix spectroscopy. Mar. Chem. 51, 325–346.

Coble, P.G., Green, S.A., Blough, N.V., Gagosian, R.B., 1990. Characterisation of dissolved organic matter in the Black Sea by fluorescence spectroscopy. Nature 348, 432–435.

Coble, P.G., Del Castillo, C.E., Avril, B., 1998. Distribution and optical properties of CDOM in the Arabian Sea during the 1995 Southwest Monsoon. Deep-Sea Res., Part 2 45, 2195–2223.

da Silva, J.C.G.E., Leitao, J.M.M., Costa, F.S., Ribeiro, J.L.A., 2002. Detection of verapamil drug by fluorescence and trilinear decomposition techniques. Anal. Chim. Acta 453 (1), 105–115.

De Souza Sierra, M.M., Donard, O.X.F., Lame, M., Beeline, C., Ewald, M., 1994. Fluorescence spectroscopy of coastal and marine waters. Mar. Chem. 47, 127–144.

Determann, S., Reuter, R., Wagner, P., Willkomm, R., 1994. Fluorescent matter in the eastern Atlantic Ocean: Part 1. Method of measurement and near-surface distribution. Deep-Sea Res., Part 1 41, 659–675.

Determann, S., Reuter, R., Willkomm, R., 1996. Fluorescent matter in the eastern Atlantic Ocean: Part 2. Vertical distribution and relation to water masses. Deep-Sea Res., Part 1 43, 345–360.

Diamond, S.A., Mount, D.R., Burkhard, L.P., Ankley, G.T., Makynen, E.A., Leonard, E.N., 2000. Effect of irradiance spectra on the photoinduced toxicity of three polycyclic aromatic hydrocarbons. Environ. Toxicol. Chem. 19, 1389–1396.

Ferreira, M.M.C., Brandes, M.L., Ferreira, I.M.C., Booksh, K.S., Dolowy, W.C., Gouterman, M., Kowalski, B.R., 1995. Chemometric study of the fluorescence of dental calculus by trilinear decomposition. Appl. Spectrosc. 49, 1317–1325.

Green, S., 1992. Applications of fluorescence spectroscopy to environmental chemistry. PhD thesis. MIT/WHOI Joint Progr. Oceanogr. 228 pp.

Harshman, R.A., 1970. Foundations of the PARAFAC procedure: model and conditions for an explanatory multi-mode factor analysis. UCLA Working papers in phonetics 16.

Harshman, R.A., Lundy, M.E., 1984. The PARAFAC model for three-way factor analysis and multidimentional scaling. In: Law, H.G., Snyder Jr., C.W., Hattie, J., McDonald, R.P. (Eds.), Research Methods for Multimode Data Analysis. Praeger, New York, pp. 122–215.

Jiji, R.D., Cooper, G.A., Booksh, K.S., 1999. Excitation–emission matrix fluorescence based determination of carbamate pesticides and polycyclic aromatic hydrocarbons. Anal. Chim. Acta 397 (1–3), 61–72.

Kalle, K., 1966. The problem of gelbstoff in the sea. Oceanogr. Mar. Biol Annu. Rev. 4, 91–104.

Lochmuller, C.H., Saavedra, S.S., 1986. Conformational changes in a soil fulvic acid measured by time dependent fluorescence depolarization. Anal. Chem. 38, 1978–1981.

McKnight, D.M., Boyer, E.W., Westerhoff, P.K., Doran, P.T., Kulbe, T., Andersen, D.T., 2001. Spectrofluorometric characterisation of dissolved organic matter for indication of precursor organic material and aromaticity. Limnol. Oceanogr. 46, 38–48.

Mobed, J.J., Hemmingsen, S.L., Autry, J.L., McGown, L.B., 1996. Fluorescence characterisation of IHSS humic substances: total luminescence spectra with absorbance correction. Environ. Sci. Technol. 30, 3061–3065.

Mopper, K., Schultz, C.A., 1993. Fluorescence as a possible tool for studying the nature and water column distribution of DOC components. Mar. Chem. 41, 238–299.

Nagata, T., 2002. Production mechanisms of dissolved organic matter. In: Kirchman, D.L. (Ed.), Microbial Ecology of the Oceans. Wiley, New York, pp. 121–152.

Opsahl, S., Benner, R., Amon, R.W., 1999. Major flux of terrige-

nous dissolved organic matter through the Arctic Ocean. Limnol. Oceanogr. 44, 2017–2023.

Persson, T., Wedborg, M., 2001. Multivariate evaluation of the fluorescence of aquatic organic matter. Anal. Chim. Acta 434, 179–192.

Ross, R.T., Lee, C., Davis, C.M., Ezzeddine, B.M., Fayyad, E.A., Leurgans, S.E., 1991. Resolution of the fluorescence spectra of plant pigment complexes using trilinear models. Biochim. Biophys. Acta 1056, 317–320.

Sharma, A., Schulman, S.G., 1999. Introduction to Fluorescence Spectroscopy. Wiley, New York.

Sidiropoulos, N.D., Bro, R., 2000. On the uniqueness of multilinear decomposition of N-way arrays. J. Chemom. 14 (3), 229–239.

Søndergaard, M., Borch, N.H., Riemann, B., 2000. Dynamics of biodegradable DOC produced by freshwater plankton communities. Aquat. Microb. Ecol. 23, 73–83.

Stedmon, C.A., Markager, S., 2001. The optics of chromophoric dissolved organic matter (CDOM) in the Greenland Sea: an algorithm for the differentiation between marine and terrestrially derived organic matter. Limnol. Oceanogr. 46, 2087–2093.

Vodacek, A., Hoge, F.E., Swift, R.N., Yungel, J.K., Peltzer, E.T., Blough, N.V., 1995. The use of in situ and airborne fluorescence measurements to determine UV absorption coefficients and DOC concentrations in surface waters. Limnol. Oceanogr. 40, 411–415.

Wang, Y.D., Borgen, O.S., Kowalski, B.R., Gu, M., Turecek, F., 1993. Advances in 2nd-order calibration. J. Chemom. 7 (2), 117–130.

Williamson, C.E., Neale, P.J., Grad, G., De Lange, H.J., Hargreaves, B.R., 2001. Beneficial and detrimental effects of UV on aquatic organisms: implications of spectral variation. Ecol. Appl. 11, 1843–1857.